MJFAS
Malaysian Journal of Fundamental and Applied Sciences

Liu *et al.* | Malaysian Journal of Fundamental and Applied Sciences, Vol. 20 (2024) 1109-1123

RESEARCH ARTICLE

Galerkin's Method and Multivariate Newton's Method for the Nonlinear Deformation of the Magneto-Electro-Elastic Bi-Layered Laminates

Mei-Feng Liu, Liew Siaw Ching*

Department of Mathematics and Applied Mathematics, Xiamen University Malaysia, Selangor, 43900, Malaysia

Abstract In this paper, mathematical modelling for the large deformation of a magneto-electro-elastic rectangular bi-layered laminate with general boundary conditions is presented. Constitutive equations involving the magneto-electro-elastic (MEE) material properties are introduced, Maxwell equations accounts for the electric and magnetic effects are also utilized. First-order shear deformation theory (FSDT) considering the von Karman nonlinear strain is adopted, and the plain strain/stress assumption applicable for thin plate analysis is used. A rather compact set of governing equations related to kinematical variables, electric/magnetic potentials and the Airy stress function is obtained as a consequence of the preliminary condensation for the electro-magnetic state to the plate kinematics. Semi-analytic solution for a bi-layered BaTiO3-CoFe2O4 laminate with specified boundary conditions subjected to various external applied loads is performed. By employing the Bubnov-Galerkin method, the set of nonlinear partial differential equations is transformed to a set of third-order nonlinear algebraic equations for the static deformation due to applied load. Numerical results are carried out by using the multivariate Newton's method with respect to various volume fractions indicating the volume ratio between piezoelectric BaTiO3 layer and piezomagnetic CoFe2O4. From the result, the nonlinearity of the von Karman strain appears to enhance system rigidity as smaller deformations will be detected when external load is applied. Also, some other interesting results are obtained which could be useful to future analysis and design of multiphase composite plates.

Keywords: Magneto-electro-elastic, Von Karman nonlinear strain, deformable theory, Bubnov-Galerkin method, multivariate Newton's method.

Introduction

Smart material made of the composition using piezoelectric and piezomagnetic components, either fiber-reinforced or layered, are generally referred as the magneto-electro-elastic material. The MEE material possess the multiphase mechanism, which can enable the energy conversion among magnetism, electricity and elasticity within the structure, and is found to have a wide range of application in various engineering fields. As one of the common seen structure type in engineering science, plate structure has drawn a lot research attraction in either the dynamic or static behaviour while it is under a certain type of applied load.

A rather compact governing equation for the magneto-electro-elastic rectangular plate is proposed by Liu [1], in which the exact solutions for the deformation of fibre-reinforced BaTiO3/CoFe2O4 composites subjected to various loads are analytically obtained based on the Kirchhoff thin-plate theory. Later on, by adopting the von Karman strain for the geometry nonlinearity, large deflection of a rectangular magneto-electro-elastic thin plate under transverse static load is investigated by Xue and colleagues [2], in which simply-supported boundary conditions are considered and coupling effect on the deflection are examined. Furthermore, by employing the first order shear deformation theory in accordance with von Karman stress function, a model for the large deflection of magneto-electro-elastic tri-layered laminate is derived by Milazzo [3]. Closed form solution for the simply-supported plate to a set of partial differential

***For correspondence:**
siawching87@yahoo.com

Received: 31 Jan. 2024
Accepted: 04 Sept. 2024

equations involving kinematical variables and stress function is presented, numerical results are carried out for various composition between the piezoelectric BaTiO3 and piezomagnetic CoFe2O4 layers with respect to different thickness ratio. Recently, the nonlinear free vibration of a symmetrically stacked MEE laminates with simply supported boundary conditions and close-circuit electro-magnetic conditions is studied by Razavi and Shooshtari [4]. As expected, by using the Galerkin's method, nonlinear governing equations are transformed into a set of coupled nonlinear ordinary differential equations with quadratic and cubic nonlinear terms. Perturbation method along time variable is used, and closed-form solution for the nonlinear frequency ratio is obtained. Also, Nazargah and Cheraghi [5] have presented a three-dimensional solution for the bending analysis of functionally graded and layered neutral magneto-electro-elastic plates resting on two-parameter elastic foundations with considering imperfect interfacial bonding. In this study, equations of motion, Gauss' equations for electrostatics and magnetostatics, boundary and interface conditions are introduced and the interfacial imperfection is modelled as a generalized spring layer.

The investigation on the composite structure comprising of a ferroelectric and a magnetostrictive material is performed by Subhani and co-workers [6], in which experimental setup for both electrical loading and magnetic loading are deployed. In this work, theoretical model for the constitutive relations in a thermodynamical framework has been proposed and the simulation results for magneto-electric composites for different volume fractions are presented. Also, a study of electro-magneto-thermoelastic interactions under Green-Naghdi theory-III of generalized thermoelasticity in the presence of initial stress is conducted by Biswas and Dahab [7]. In their study, fundamental equations of the two-dimensional problem in orthotropic medium under the influence of electric and magnetic field are obtained in the form of vector-matrix for differential equation by employing the normal mode analysis. The solution for temperature distribution, displacements, and stress components is obtained by utilizing the method of eigenfunction expansion, and the effect of magnetic field, electric field and phase velocity are displayed.

Since most of the literature available are dealing with the plates or laminate with simply-supported boundary conditions, this gives rise the desire to investigate the related behaviors of MEE plate under the other type of boundary conditions such as clamped around or cantilever one. The purpose of the present study is to develop a general expression for the solution to the large deformation of MEE bi-layered laminates with general boundary conditions and subject to various mechanical loading. In this work, multivariate Newton's method is used to solve nonlinear algebraic equations arising from the implementation of Bubnov-Galerkin's method on the nonlinear governing equation via collecting multiple terms of the generalized Fourier series solution. It is well known that Galerkin's method is a family of methods converting continuous differential operators into discrete linear/nonlinear system by applying finite sets of basis functions with certain constraints as the approximate solutions. When referring to Galerkin method, which is named after the Soviet mathematician Boris Galerkin, three major categories are brought out, they are respectively Ritz-Galerkin method (named after Walther Ritz), Bubnov-Galerkin method (named after Ivan Bubnov) and Petrov-Galerkin method (named after Georgii I. Petrov). Based on the nonlinearity of the proposed governing equation, Bubnov version of the Galerkin method is adopted in the present study, meanwhile, the weighting functions are chosen to be the same as the orthogonal basis functions as expected. A schematic procedure has been clearly specified and the related nonlinear terms are successfully resolved by introducing new index in the summation notation, furthermore, 3D visualization about the nonlinear effect on the static deformation of the MEE plate has been graphically presented, which is never seen in the existing available literature.

In this paper, first-order shear deformation as well as the von Karman nonlinear strain will be adopted as usual, plain strain/stress assumption applicable for thin plate analysis is also suggested. The governing equations related to the kinematical variables, electric/magnetic potentials are therefore derived, and the set of nonlinear partial differential equations will be transformed to a set of cubic nonlinear algebraic equations by using Galerkin's method. The proposed mathematical formulation is based on the first-order shear deformable theory (FSDT), which is a classical model for thin plate analysis, and it is not suitable for the analysis of thick magneto-electro-elastic laminates. Therefore, the current frame of work will be restricted to rather thin MEE plates or laminates with the ratio of thickness to span less than 1/10. Numerical results will be carried out through the multivariate Newton's method, the effect of volume fraction between piezoelectric BaTiO3 and piezomagnetic CoFe2O4 continua on the large deformation plate are further investigated.

Formulation

Governing Equations

Consider the Cartesian coordinate (*x*, *y*, *z*) as indicated in Figure 1 below, and let the bi-layered

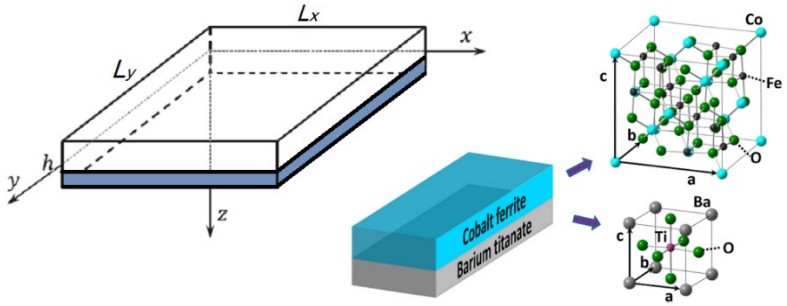

Figure 1. Physical model of the magneto-electro-elastic bi-layered laminate

BaTiO3/CoFe2O4 laminate be modelled as a transversely isotropic thin plate, the constitutive equations for the bending problem of a thin MEE plate based on both the plane strain and plane stress assumptions in accordance with the non-zero transverse fields can be expressed as Liu [1],

$$\sigma_x = c_{11}\varepsilon_x + c_{12}\varepsilon_y + e_{31}\frac{\partial\phi}{\partial z} + q_{31}\frac{\partial\psi}{\partial z} \quad (1)$$

$$\sigma_y = c_{12}\varepsilon_x + c_{11}\varepsilon_y + e_{31}\frac{\partial\phi}{\partial z} + q_{31}\frac{\partial\psi}{\partial z} \quad (2)$$

$$\tau_{xy} = c_{66}\gamma_{xy} \quad (3)$$

$$D_z = e_{31}\varepsilon_x + e_{31}\varepsilon_y - \kappa_{33}\frac{\partial\phi}{\partial z} - d_{33}\frac{\partial\psi}{\partial z} \quad (4)$$

$$B_z = q_{31}\varepsilon_x + q_{31}\varepsilon_y - d_{33}\frac{\partial\phi}{\partial z} - \mu_{33}\frac{\partial\psi}{\partial z} \quad (5)$$

where σ_x, σ_y and τ_{xy} are the normal and shear stresses, ε_x, ε_y and γ_{xy} are the corresponding normal and shear strains, D_z and B_z denote the electric and magnetic displacements along transverse direction, ϕ and ψ are the electric and magnetic potentials. The other parameters are all material constants, among which c_{11}, c_{12}, c_{66} are the elastic constants, e_{31} is the piezo-elastic constant, q_{31} is the piezo-magnetic constant, κ_{33} is the dielectric constant, d_{33} is the magneto-electric constant and μ_{33} is the magnetic constant, respectively.

By adopting the von Karman nonlinear strain for large deflection of plates, the following strain-displacement relations are introduced by Reddy [8]

$$\varepsilon_x = \frac{\partial u}{\partial x} + \frac{1}{2}\left(\frac{\partial w}{\partial x}\right)^2 \quad (6)$$

$$\varepsilon_y = \frac{\partial v}{\partial y} + \frac{1}{2}\left(\frac{\partial w}{\partial y}\right)^2 \quad (7)$$

$$\gamma_{xy} = \frac{\partial v}{\partial x} + \frac{\partial u}{\partial y} + \frac{\partial w}{\partial x}\cdot\frac{\partial w}{\partial y} \quad (8)$$

where u, v and w are the elastic displacement components in the x-, y- and z- directions, respectively.

Based on the assumption valid for thin plate structures [1, 9], one can ignore the in-plane electric and magnetic fields and only focus on the transverse electric field E_z and magnetic field H_z, which relates the electric potential ϕ and magnetic potential ψ by the following Maxwell equations:

$$E_z = -\frac{\partial\phi}{\partial z}, H_z = -\frac{\partial\psi}{\partial z}.$$

Furthermore, according to the equilibrium equations of electric charge and current, the electric and magnetic potentials can be solved analytically in terms of the material parameters and transverse deflection of the deformed plate by [1, 2]

$$\frac{\partial \phi}{\partial z} = -\frac{\Delta_1}{\Delta} z\nabla^2 w + \phi_1(x,y) \tag{9}$$
$$\frac{\partial \psi}{\partial z} = -\frac{\Delta_2}{\Delta} z\nabla^2 w + \psi_1(x,y) \tag{10}$$

where $\phi_1(x,y)$ and $\psi_1(x,y)$ represent the variations of electric field and magnetic field in the thickness direction while the plate is deformed, and the related parameter are defined as

$$\Delta \equiv \det\begin{bmatrix}\kappa_{33} & d_{33}\\ d_{33} & \mu_{33}\end{bmatrix},\ \Delta_1 \equiv \det\begin{bmatrix}e_{31} & d_{33}\\ q_{31} & \mu_{33}\end{bmatrix},\ \Delta_2 \equiv \det\begin{bmatrix}\kappa_{33} & e_{31}\\ d_{33} & q_{31}\end{bmatrix}.$$

It should be noted that for closed-circuit condition are under consideration, it implies that [1]

$$\phi_1(x,y) = \psi_1(x,y) = 0.$$

Recalling that the resultant forces and moments are defined as follows

$$N_x = \int_{-h/2}^{h/2} \sigma_x\, dz,\ N_y = \int_{-h/2}^{h/2} \sigma_y\, dz,\ N_{xy} = \int_{-h/2}^{h/2} \tau_{xy}\, dz;$$
$$M_x = \int_{-h/2}^{h/2} \sigma_x z\, dz,\ M_y = \int_{-h/2}^{h/2} \sigma_y z\, dz,\ M_{xy} = \int_{-h/2}^{h/2} \tau_{xy} z\, dz,$$

and equation of static equilibrium for bending plate can be given by

$$\frac{\partial^2 M_x}{\partial x^2} + 2\frac{\partial^2 M_{xy}}{\partial x \partial y} + \frac{\partial^2 M_y}{\partial y^2} + N_x\frac{\partial^2 w}{\partial x^2} + N_y\frac{\partial^2 w}{\partial y^2} + 2N_{xy}\frac{\partial^2 w}{\partial x \partial y} + \Delta q(x,y) = 0, \tag{11}$$

where $\Delta q(x,y) \equiv q_{\text{upper}}(x,y) - q_{\text{lower}}(x,y)$ denotes the difference of applied load between top surface and bottom surface of the plate.

Substituting Eq. (6)-(10) into Eq. (1)-(3) and integrate them along the thickness direction lead to the following

$$M_x = -\frac{h^3}{12}\left[c_{11}\frac{\partial^2 w(x,y)}{\partial x^2} + c_{12}\frac{\partial^2 w(x,y)}{\partial y^2} + e_{31}\frac{\Delta_1}{\Delta}\nabla^2 w + q_{31}\frac{\Delta_2}{\Delta}\nabla^2 w\right],$$
$$M_y = -\frac{h^3}{12}\left[c_{12}\frac{\partial^2 w(x,y)}{\partial x^2} + c_{11}\frac{\partial^2 w(x,y)}{\partial y^2} + e_{31}\frac{\Delta_1}{\Delta}\nabla^2 w + q_{31}\frac{\Delta_2}{\Delta}\nabla^2 w\right],$$
$$M_{xy} = -\frac{h^3}{12}\cdot 2c_{66}\frac{\partial^2 w(x,y)}{\partial x \partial y},$$
$$N_x = h\left\{c_{11}\left[\frac{\partial u_0(x,y)}{\partial x} + \frac{1}{2}\left(\frac{\partial w}{\partial x}\right)^2\right] + c_{12}\left[\frac{\partial v_0(x,y)}{\partial y} + \frac{1}{2}\left(\frac{\partial w}{\partial y}\right)^2\right] + e_{31}\phi_1(x,y) + q_{31}\psi_1(x,y)\right\},$$
$$N_y = h\left\{c_{12}\left[\frac{\partial u_0(x,y)}{\partial x} + \frac{1}{2}\left(\frac{\partial w}{\partial x}\right)^2\right] + c_{11}\left[\frac{\partial v_0(x,y)}{\partial y} + \frac{1}{2}\left(\frac{\partial w}{\partial y}\right)^2\right] + e_{31}\phi_1(x,y) + q_{31}\psi_1(x,y)\right\},$$
$$N_{xy} = h\left\{c_{66}\left[\frac{\partial v_0(x,y)}{\partial x} + \frac{\partial u_0(x,y)}{\partial y} + \frac{\partial w}{\partial x}\frac{\partial w}{\partial y}\right]\right\}.$$

Therefore, the governing equation for bending deformation of a MEE plate can be derived as follows

$$\frac{h^3}{12}\left(c_{11} + e_{31}\frac{\Delta_1}{\Delta} + q_{31}\frac{\Delta_2}{\Delta}\right)\nabla^4 w = \Delta q(x,y) + h\left\{\frac{1}{2}\left[c_{11}\left(\frac{\partial w}{\partial x}\right)^2 + c_{12}\left(\frac{\partial w}{\partial y}\right)^2\right]\frac{\partial^2 w}{\partial x^2} + \frac{1}{2}\left[c_{12}\left(\frac{\partial w}{\partial x}\right)^2 + c_{11}\left(\frac{\partial w}{\partial y}\right)^2\right]\frac{\partial^2 w}{\partial y^2} + 2c_{66}\frac{\partial w}{\partial x}\frac{\partial w}{\partial y}\frac{\partial^2 w}{\partial x \partial y} + [e_{31}\phi_1(x,y) + q_{31}\psi_1(x,y)]\frac{\partial^2 w}{\partial x^2} + [e_{31}\phi_1(x,y) + q_{31}\psi_1(x,y)]\frac{\partial^2 w}{\partial y^2}\right\}. \tag{12}$$

And it could be further simplified if additional material parameter is defined

$$\left(D_E + D_{\text{pz}} + D_{\text{pm}}\right)\nabla^4 w = \Delta q(x,y) + h\left\{\frac{1}{2}c_{12}\nabla^2 w\cdot\nabla^2 w + c_{66}\left[\left(\frac{\partial w}{\partial x}\right)^2\frac{\partial^2 w}{\partial x^2} + 2\frac{\partial w}{\partial x}\frac{\partial w}{\partial y}\frac{\partial^2 w}{\partial x \partial y} + \left(\frac{\partial w}{\partial y}\right)^2\frac{\partial^2 w}{\partial y^2}\right] + [e_{31}\phi_1(x,y) + q_{31}\psi_1(x,y)]\cdot\nabla^2 w\right\} \tag{13}$$

where

$$D_E \equiv \frac{c_{11}h^3}{12},\ D_{\text{pz}} \equiv \frac{h^3}{12}e_{31}\frac{\Delta_1}{\Delta},\ D_{\text{pm}} \equiv \frac{h^3}{12}q_{31}\frac{\Delta_2}{\Delta}$$

represent the plate elastic rigidity, piezoelectric rigidity and piezomagnetic rigidity, respectively. It should be noted that the relation $c_{11} = c_{12} + 2c_{66}$ has been used in the above derivation.

Solution Method

In seeking for the solution of nonlinear governing equation mentioned above, we can assume the following expression as the transverse deflection of the MEE plate

$$w(x,y) = \sum_{m=1}^{\infty}\sum_{n=1}^{\infty} A_{mn} X_m(x)\, Y_n(y) \tag{14}$$

where $X_m(x)$ and $Y_n(y)$ are homogeneous solution of Eq. (13) and be determined according to the specified boundary conditions. Some commonly seen mode shapes and the corresponding eigenvalues with respect to various boundary conditions are tabulated in Table 1 as below. It should be noted that

Table 1. Mode shapes and the corresponding eigenvalues for specified boundary conditions

Boundary Conditions	Mode shape $X_m(\xi)$	Eigenvalues α_m
Pinned-Pinned	$X_m(\xi) = \sin\left(\frac{m\pi}{L}\right)\xi$	$\alpha_m = \frac{m\pi}{L_x}, m = 1,2,3,...$
Fixed-Pined	$X_m(\xi) = \cosh\alpha_m\xi - \cos\alpha_m\xi - \gamma_m(\sinh\alpha_m\xi - \sin\alpha_m\xi)$ where $\gamma_1 = 1.000777$, $\gamma_2 = 1.000001$, $\gamma_3 = 1.000000$	$\alpha_1 = \frac{3.926602}{L}$, $\alpha_2 = \frac{7.068583}{L}$, $\alpha_3 = \frac{10.210176}{L}$
Fixed-Free	$X_m(\xi) = \cosh\alpha_m\xi - \cos\alpha_m\xi - \gamma_m(\sinh\alpha_m\xi - \sin\alpha_m\xi)$ where $\gamma_1 = 0.734096$, $\gamma_2 = 1.018466$, $\gamma_3 = 0.999225$	$\alpha_1 = \frac{1.875104}{L}$, $\alpha_2 = \frac{4.694091}{L}$, $\alpha_3 = \frac{7.854757}{L}$
Fixed-Fixed	$X_m(\xi) = \cosh\alpha_m\xi - \cos\alpha_m\xi - \gamma_m(\sinh\alpha_m\xi - \sin\alpha_m\xi)$ where $\gamma_1 = 0.982502$, $\gamma_2 = 1.000777$, $\gamma_3 = 0.999966$	$\alpha_1 = \frac{4.730041}{L_x}$, $\alpha_2 = \frac{7.853205}{L_x}$, $\alpha_3 = \frac{10.995607}{L_x}$
Free-Free	$X_m(\xi) = \cosh\alpha_m\xi + \cos\alpha_m\xi - \gamma_m(\sinh\alpha_m\xi + \sin\alpha_m\xi)$ where $\gamma_1 = 0.982502$, $\gamma_2 = 1.000777$, $\gamma_3 = 0.999966$	$\alpha_1 = \frac{4.730041}{L_x}$, $\alpha_2 = \frac{7.853205}{L_x}$, $\alpha_3 = \frac{10.995607}{L_x}$

the mode shapes $X_m(x)$ and $Y_n(y)$ are chosen in the way satisfying the corresponding boundary conditions and also the function orthogonality.

After $X_m(x)$ and $Y_n(y)$ are determined, we can further expand the applied load on the top or bottom surface of the plate into the generalized double Fourier series as

$$\Delta q(x,y) = \sum_{m=1}^{\infty}\sum_{n=1}^{\infty} Q_{mn} X_m(x)\, Y_n(y). \tag{15}$$

By substituting Eq. (14) and Eq. (15) into Eq.(13), we can have the following equation:

$$\sum_{m=1}^{\infty}\sum_{n=1}^{\infty}A_{mn}\{(D+E+M)(\alpha_m^4+2\alpha_m^2\beta_n^2+\beta_n^4)-h[e_{31}\phi_1(x,y)+q_{31}\psi_1(x,y)](\alpha_m^2+\beta_n^2)\}X_m(x)\,Y_n(y)=\sum_{m=1}^{\infty}\sum_{n=1}^{\infty}Q_{mn}X_m(x)Y_n(y)+\frac{h}{2}\Big\{c_{11}\Big[\Big(\sum_{m=1}^{\infty}\sum_{n=1}^{\infty}A_{mn}\alpha_m X_m(x)Y_n(y)\Big)^2+\Big(\sum_{m=1}^{\infty}\sum_{n=1}^{\infty}A_{mn}\beta_n\ X_m(x)Y_n(y)\Big)^2\Big]\Big(\sum_{m=1}^{\infty}\sum_{n=1}^{\infty}A_{mn}(\alpha_m^2+\beta_n^2)\,X_m(x)Y_n(y)\Big)\Big\}-h\Big\{c_{66}\Big[\Big(\sum_{m=1}^{\infty}\sum_{n=1}^{\infty}A_{mn}\beta_n\ X_m(x)Y_n(y)\Big)^2\Big(\sum_{m=1}^{\infty}\sum_{n=1}^{\infty}A_{mn}\alpha_m^2X_m(x)Y_n(y)\Big)+\Big(\sum_{m=1}^{\infty}\sum_{n=1}^{\infty}A_{mn}\alpha_m X_m(x)Y_n(y)\Big)^2\Big(\sum_{m=1}^{\infty}\sum_{n=1}^{\infty}A_{mn}\beta_n^2\,X_m(x)Y_n(y)\Big)\Big]\Big\}+2hc_{66}\Big(\sum_{m=1}^{\infty}\sum_{n=1}^{\infty}A_{mn}\alpha_m X_m(x)\,Y_n(y)\Big)\Big(\sum_{m=1}^{\infty}\sum_{n=1}^{\infty}A_{mn}\beta_n\ X_m(x)Y_n\ (y)\Big)\Big(\sum_{m=1}^{\infty}\sum_{n=1}^{\infty}A_{mn}\alpha_m\beta_n\ X_m(x)\,Y_n\ (y)\Big)$$

where α_m and β_n refer to the eigenvalues for the corresponding boundary conditions. By introducing new index for the summation in nonlinear terms to avoid duplication, the right hand side of the above equation will be further expressed as

$$\sum_{m=1}^{\infty}\sum_{n=1}^{\infty}Q_{mn}X_m(x)Y_n(y)+\frac{h}{2}c_{11}\Big(\sum_{i=1}^{\infty}\sum_{j=1}^{\infty}A_{ij}\alpha_i\ X_i(x)Y_j(y)\Big)\Big(\sum_{k=1}^{\infty}\sum_{l=1}^{\infty}A_{kl}\alpha_k\ X_k(x)Y_l(y)\Big)\Big(\sum_{m=1}^{\infty}\sum_{n=1}^{\infty}A_{mn}(\alpha_m^2+\beta_n^2)\,X_m(x)Y_n(y)\Big)-hc_{66}\Big(\sum_{i=1}^{\infty}\sum_{j=1}^{\infty}A_{ij}\alpha_i\ X_i(x)Y_j(y)\Big)\Big(\sum_{k=1}^{\infty}\sum_{l=1}^{\infty}A_{kl}\alpha_k\ X_k(x)Y_l(y)\Big)\Big(\sum_{m=1}^{\infty}\sum_{n=1}^{\infty}A_{mn}\beta_n^2\,X_m(x)Y_n(y)\Big)+\frac{h}{2}c_{11}\Big(\sum_{i=1}^{\infty}\sum_{j=1}^{\infty}A_{ij}\beta_j\ X_i(x)Y_j(y)\Big)\Big(\sum_{k=1}^{\infty}\sum_{l=1}^{\infty}A_{kl}\beta_l\ X_k(x)Y_l(y)\Big)\Big(\sum_{m=1}^{\infty}\sum_{n=1}^{\infty}A_{mn}(\alpha_m^2+\beta_n^2)\,X_m(x)Y_n(y)\Big)-hc_{66}\Big(\sum_{i=1}^{\infty}\sum_{j=1}^{\infty}A_{ij}\beta_j\ X_i(x)Y_j(y)\Big)\Big(\sum_{k=1}^{\infty}\sum_{l=1}^{\infty}A_{kl}\beta_l\ X_k(x)Y_l(y)\Big)\Big(\sum_{m=1}^{\infty}\sum_{n=1}^{\infty}A_{mn}\alpha_m^2X_m(x)Y_n(y)\Big)+2hc_{66}\Big(\sum_{m=1}^{\infty}\sum_{n=1}^{\infty}A_{mn}\alpha_m X_m(x)\,Y_n(y)\Big)\Big(\sum_{m=1}^{\infty}\sum_{n=1}^{\infty}A_{mn}\beta_n\ X_m(x)Y_n\ (y)\Big)\Big(\sum_{m=1}^{\infty}\sum_{n=1}^{\infty}A_{mn}\alpha_m\beta_n\ X_m(x)\,Y_n\ (y)\Big).$$

Implementing Galerkin's method on the governing equation by integrating it with the weighting function which is chosen to be the same as the shape function, the following equation set can be obtained for $p,q=1,2,3\cdots$:

$$A_{pq}\{(D+E+M)(\alpha_p^4+2\alpha_p^2\beta_q^2+\beta_q^4)-h[e_{31}\phi_1(x,y)+q_{31}\psi_1(x,y)](\alpha_p^2+\beta_q^2)\}\|X_p(x)\|\|Y_q(y)\|=Q_{pq}\|X_p(x)\|\|Y_q(y)\|+\frac{h}{2}c_{11}\sum_{i=1}^{\infty}\sum_{j=1}^{\infty}\sum_{k=1}^{\infty}\sum_{l=1}^{\infty}\sum_{m=1}^{\infty}\sum_{n=1}^{\infty}A_{ij}A_{kl}A_{mn}\alpha_i\ \alpha_k\ (\alpha_m^2+\beta_n^2)\,\|X_{ikmp}(x)\|\|Y_{jlnq}(y)\|-hc_{66}\sum_{i=1}^{\infty}\sum_{j=1}^{\infty}\sum_{k=1}^{\infty}\sum_{l=1}^{\infty}\sum_{m=1}^{\infty}\sum_{n=1}^{\infty}A_{ij}A_{kl}A_{mn}\alpha_i\ \alpha_k\ \beta_n^2\,\|X_{ikmp}(x)\|\|Y_{jlnq}(y)\|+\frac{h}{2}c_{11}\sum_{i=1}^{\infty}\sum_{j=1}^{\infty}\sum_{k=1}^{\infty}\sum_{l=1}^{\infty}\sum_{m=1}^{\infty}\sum_{n=1}^{\infty}A_{ij}A_{kl}A_{mn}\beta_j\ \beta_l\ (\alpha_m^2+\beta_n^2)\,\|X_{ikmp}(x)\|\|Y_{jlnq}(y)\|-hc_{66}\sum_{i=1}^{\infty}\sum_{j=1}^{\infty}\sum_{k=1}^{\infty}\sum_{l=1}^{\infty}\sum_{m=1}^{\infty}\sum_{n=1}^{\infty}A_{ij}A_{kl}A_{mn}\beta_j\ \beta_l\ \alpha_m^2\,\|X_{ikmp}(x)\|\|Y_{jlnq}(y)\|+2hc_{66}\sum_{i=1}^{\infty}\sum_{j=1}^{\infty}\sum_{k=1}^{\infty}\sum_{l=1}^{\infty}\sum_{m=1}^{\infty}\sum_{n=1}^{\infty}A_{ij}A_{kl}A_{mn}\alpha_i\ \beta_l\ \alpha_m\beta_n\ \|X_{ikmp}(x)\|\|Y_{jlnq}(y)\|$$

where $\|X_p(x)\|\equiv\int_0^{L_x}X_p(x)^2\,dx$ and $\|Y_q(y)\|\equiv\int_0^{L_x}X_q(x)^2\,dx$ are the conventional 2-norm for functions and it is worth of noting that an additional nonlinear norm are defined in the following fashion

$$\|X_{ikmp}(x)\|\equiv\int_0^{L_x}X_i(x)X_k(x)X_m(x)\,X_p(x)dx,$$
$$\|Y_{jlnq}(y)\|\equiv\int_0^{L_y}Y_j(y)Y_l(y)Y_n(y)\,Y_q(y)dy.$$

Even though it looks very complicated, however, the whole system is merely a set of nonlinear equations in terms of the Fourier Series coefficient A_{ij} as stated as follows

$$(A_{ij})=F_{ij}(A_{ij}),\ \text{for } i=1,2,\cdots M;\ \ j=1,2,\cdots,N$$

or alternatively

$$\mathbf{A}_{M\times N}=\mathbf{F}_{M\times N}(\mathbf{A}_{M\times N})$$

which is only a set of nonlinear algebraic equations and can be solved numerically by using the multi-variate Newton's method in this study.

Multivariate Newton's Method

For the specified integers p and q, where $p = 1,2,\cdots,M$, and $q = 1,2,\cdots,N$, the governing equation can be converted into the following form after adopting Galerkin's method

$$A_{pq}\{(D+E+M)(\alpha_p^4+2\alpha_p^2\beta_q^2+\beta_q^4)-h[e_{31}\phi_0(x,y)+q_{31}\psi_0(x,y)](\alpha_p^2+\beta_q^2)\}\|X_p(x)\|\|Y_q(y)\| = Q_{pq}\|X_p(x)\|\|Y_q(y)\|+\frac{h}{2}c_{11}\sum_{i=1}^{\infty}\sum_{j=1}^{\infty}\sum_{k=1}^{\infty}\sum_{l=1}^{\infty}\sum_{m=1}^{\infty}\sum_{n=1}^{\infty}A_{ij}A_{kl}A_{mn}\alpha_i\ \alpha_k\ (\alpha_m^2+\beta_n^2)\ \|X_{ikmp}(x)\|\|Y_{jlnq}(y)\|-hc_{66}\sum_{i=1}^{\infty}\sum_{j=1}^{\infty}\sum_{k=1}^{\infty}\sum_{l=1}^{\infty}\sum_{m=1}^{\infty}\sum_{n=1}^{\infty}A_{ij}A_{kl}A_{mn}\alpha_i\ \alpha_k\ \beta_n^2\ \|X_{ikmp}(x)\|\|Y_{jlnq}(y)\|+\frac{h}{2}c_{11}\sum_{i=1}^{\infty}\sum_{j=1}^{\infty}\sum_{k=1}^{\infty}\sum_{l=1}^{\infty}\sum_{m=1}^{\infty}\sum_{n=1}^{\infty}A_{ij}A_{kl}A_{mn}\beta_j\ \beta_l\ (\alpha_m^2+\beta_n^2)\ \|X_{ikmp}(x)\|\|Y_{jlnq}(y)\|-hc_{66}\sum_{i=1}^{\infty}\sum_{j=1}^{\infty}\sum_{k=1}^{\infty}\sum_{l=1}^{\infty}\sum_{m=1}^{\infty}\sum_{n=1}^{\infty}A_{ij}A_{kl}A_{mn}\beta_j\ \beta_l\ \alpha_m^2\ \|X_{ikmp}(x)\|\|Y_{jlnq}(y)\|+2hc_{66}\sum_{i=1}^{\infty}\sum_{j=1}^{\infty}\sum_{k=1}^{\infty}\sum_{l=1}^{\infty}\sum_{m=1}^{\infty}\sum_{n=1}^{\infty}A_{ij}A_{kl}A_{mn}\alpha_i\ \beta_l\ \alpha_m\beta_n\ \|X_{ikmp}(x)\|\|Y_{jlnq}(y)\| \quad (16)$$

In order to simplify the computation for finding out the coefficients A_{pq}, the following index notations are invented. First set the new index *L* to b

$$L = (p-1)\cdot N + q \quad (17)$$

thus we can convert the matrix into vector as

$$(A_{pq}) = (A_L),\ L = 1,2,\cdots MN$$

and the retrieving equation will be

$$p = \left\lceil \frac{L}{N} \right\rceil,\ q = (L-1)|N+1$$

where $\lceil(\cdot)\rceil$ denotes the Least Integer Function and $(\cdot)|N$ is the modulus of N. Next we can use the same philosophy to set the following indexes in order to reduce the dimension

$$I = (i-1)\cdot N + j \implies i = \left\lceil \frac{I}{N} \right\rceil, j = (I-1)|N+1$$
$$J = (k-1)\cdot N + l \implies k = \left\lceil \frac{J}{N} \right\rceil, l = (J-1)|N+1$$
$$K = (m-1)\cdot N + n \implies m = \left\lceil \frac{K}{N} \right\rceil, n = (K-1)|N+1.$$

By introducing the above notation, Eq. (16) can be re-written as

$$A_L\{(D+E+M)\Lambda_L^4-h[e_{31}\phi_0(x,y)+q_{31}\psi_0(x,y)]\Lambda_L^2\}\|XY_L\| = Q_L\|XY_L\|+\frac{h}{2}c_{11}\sum_{I=1}^{MN}\sum_{J=1}^{MN}\sum_{K=1}^{MN} A_IA_JA_K\alpha_{\left\lceil \frac{I}{N} \right\rceil}\alpha_{\left\lceil \frac{J}{N} \right\rceil}\Lambda_K^2\left\|XY_{IJKL}\right\|_3-hc_{66}\sum_{I=1}^{MN}\sum_{J=1}^{MN}\sum_{K=1}^{MN} A_IA_JA_K\ \alpha_{\left\lceil \frac{I}{N} \right\rceil}\alpha_{\left\lceil \frac{J}{N} \right\rceil}\beta_{K|N}^2\left\|XY_{IJKL}\right\|_3+\frac{h}{2}c_{11}\sum_{I=1}^{MN}\sum_{J=1}^{MN}\sum_{K=1}^{MN} A_IA_JA_K\ \beta_{I|N}\beta_{J|N}\Lambda_K^2\left\|XY_{IJKL}\right\|_3-hc_{66}\sum_{I=1}^{MN}\sum_{J=1}^{MN}\sum_{K=1}^{MN} A_IA_JA_K\ \beta_{I|N}\beta_{J|N}\alpha_{\left\lceil \frac{K}{N} \right\rceil}^2\left\|XY_{IJKL}\right\|_3+2hc_{66}\sum_{i=1}^{\infty}\sum_{j=1}^{\infty}\sum_{k=1}^{\infty}\sum_{l=1}^{\infty}\sum_{m=1}^{\infty}\sum_{n=1}^{\infty}A_IA_JA_K\alpha_{\left\lceil \frac{I}{N} \right\rceil}\beta_{(J-1)|N+1}\alpha_{\left\lceil \frac{K}{N} \right\rceil}\beta_{(K-1)|N+1}\left\|XY_{IJKL}\right\|_3 \quad (18)$$

in which some parameters are redefined as

$$\Lambda_{mn}^2 = (\alpha_m^2+\beta_n^2) = \Lambda_K^2$$
$$\Gamma_{mn}^2 = (\alpha_m^2\beta_n^2) = \Gamma_K^2$$
$$\|XY_L\| \equiv \|X_p(x)\|\|Y_q(y)\| = \left\|X_{\left\lceil \frac{L}{N} \right\rceil}(x)\right\|\|Y_{(L-1)|N+1}(y)\|$$
$$\left\|XY_{IJKL}\right\|_3 \equiv \|X_{ikmp}(x)\|\|Y_{jlnq}(y)\|.$$

As we may see from Eq. (18) that even it looks so complicate but actually it is merely a set of nonlinear equations with the following form

$$A_LC_L^0 = Q_L + G_L(A_1,A_2,\cdots,A_{MN})$$

or in matrix form to be

$$\mathbf{A}\cdot\mathbf{C}=\mathbf{Q}+\mathbf{G}(\mathbf{A})$$

furthermore, the following nonlinear system is reached for each $L=1,2,\cdots MN$

$$F_L(A_I,A_J,A_K)\colon A_LC_L^0-Q_L^0-\sum_{I=1}^{MN}\sum_{J=1}^{MN}\sum_{K=1}^{MN}\left(C_{IJKL}^1+C_{IJKL}^2+C_{IJKL}^3+C_{IJKL}^4+C_{IJKL}^5\right)A_IA_JA_K$$

i.e.,

$$F_L(A_I,A_J,A_K)\equiv A_LC_L^0-Q_L^0-\sum_{I=1}^{MN}\sum_{J=1}^{MN}\sum_{K=1}^{MN}C_{IJKL}^{\text{total}}A_IA_JA_K=0,\ \text{for } L=1,2,\cdots,MN$$

where

$$C_L^0\equiv\{(D+E+M)\Lambda_L^4-h[e_{31}\phi_1(x,y)+q_{31}\psi_1(x,y)]\Lambda_L^2\}\|XY_L\|$$
$$Q_L^0\equiv Q_L\|XY_L\|$$
$$C_{IJKL}^1\equiv\frac{h}{2}c_{11}\alpha_{\left|\frac{I}{N}\right|}\alpha_{\left|\frac{J}{N}\right|}\Lambda_K^2\left\|XY_{IJKL}\right\|_3$$
$$C_{IJKL}^2\equiv-hc_{66}\alpha_{\left|\frac{I}{N}\right|}\alpha_{\left|\frac{J}{N}\right|}\beta_{(K-1)|N+1}^2\left\|XY_{IJKL}\right\|_3$$
$$C_{IJKL}^3\equiv\frac{h}{2}c_{11}\beta_{(I-1)|N+1}\beta_{(J-1)|N+1}\Lambda_K^2\left\|XY_{IJKL}\right\|_3$$
$$C_{IJKL}^4\equiv-hc_{66}\beta_{(I-1)|N+1}\beta_{(J-1)|N+1}\alpha_{\left|\frac{K}{N}\right|}^2\left\|XY_{IJKL}\right\|_3$$
$$C_{IJKL}^5\equiv 2hc_{66}\alpha_{\left|\frac{I}{N}\right|}\beta_{(J-1)|N+1}\alpha_{\left|\frac{K}{N}\right|}\beta_{(K-1)|N+1}\left\|XY_{IJKL}\right\|_3$$
$$C_{IJKL}^{\text{total}}=C_{IJKL}^1+C_{IJKL}^2+C_{IJKL}^3+C_{IJKL}^4+C_{IJKL}^5\ .$$

For implementing the multivariate Newton's method, the Jacobian of the system is required, which will be obtained by evaluating the functions F_L with respect to all independent variables, say A_l, for $L=1,2,\cdots,MN$ and $l=1,2,\cdots,MN$,

$$\mathbf{J}\left(\frac{\boldsymbol{F}}{\mathbf{A}}\right)_{Ll}=\left(\frac{\partial F_L}{\partial A_l}\right)=\frac{\partial}{\partial A_l}\left(A_LC_L^0-Q_L^0-\sum_{I=1}^{MN}\sum_{J=1}^{MN}\sum_{K=1}^{MN}C_{IJKL}^{\text{total}}A_IA_JA_K\right)=C_l^0-0-$$
$$\left(\sum_{I=1}^{MN}\sum_{J=1}^{MN}\sum_{K=1}^{MN}C_{IJKL}^{\text{total}}\frac{\partial A_I}{\partial A_l}A_JA_K\right)-\left(\sum_{I=1}^{MN}\sum_{J=1}^{MN}\sum_{K=1}^{MN}C_{IJKL}^{\text{total}}A_I\frac{\partial A_J}{\partial A_l}A_K\right)-\left(\sum_{I=1}^{MN}\sum_{J=1}^{MN}\sum_{K=1}^{MN}C_{IJKL}^{\text{total}}A_IA_J\frac{\partial A_K}{\partial A_l}\right)=$$
$$C_l^0-\left(\sum_{I=1}^{MN}\sum_{J=1}^{MN}C_{IJlL}^{\text{total}}A_IA_J\right)-\left(\sum_{I=1}^{MN}\sum_{J=1}^{MN}C_{IJlL}^{\text{total}}A_IA_J\right)-\left(\sum_{I=1}^{MN}\sum_{J=1}^{MN}C_{IJlL}^{\text{total}}A_IA_J\right)=C_l^0-$$
$$3\sum_{I=1}^{MN}\sum_{J=1}^{MN}C_{IJlL}^{\text{total}}A_IA_J.$$

Newton's method for systems [10] is stated in Appendix A for reader's reference, it should be noted that the initial approximation in the algorithm is chosen as the linear deformation conducted by Liu [1] for the present study, and the 2-norm for $\mathbf{y}$ in stopping procedure $\|\mathbf{y}\|<TOL$ is used in the programming code.

After implementing the multivariate Newton's method, the approximation of the coefficients A_L can be obtained numerically, and further be converted back to A_{pq} through Eq.(17), therefore, the series solution for the nonlinear deformation presented in last section can be achieved, and corresponding results subjected to various type of the applied loads are illustrated in the next section.

Numerical Results and Discussions

Electric and Magnetic Boundary Conditions

The electric boundary conditions and magneto boundary conditions on the top and bottom surfaces can normally be divided into two categories, namely the Closed-Circuit conditions and Open-Circuit one, however, for the sake of simplicity only the Closed-Circuit boundary conditions is investigated in this paper.

For a closed-circuit MEE laminate, the potential on the top and bottom surfaces are

$$\phi\left(x,y,\pm\frac{h}{2}\right)=0,\ \ \psi\left(x,y,\pm\frac{h}{2}\right)=0,$$

thus, according to Eq. (9) and Eq.(10), it can be easily deduced that the variations of electric field and magnetic field along the thickness direction will vanish, i.e., we have

$\phi_1(x, y) = \psi_1(x, y) = 0.$
And the expression for the constant associated with the coefficient A_{pq} will be reduced into

$C_L^0 \equiv \{(D + E + M)\Lambda_L^4\} \| XY_L \|,$

and the following examples presented in this section will be always using the same setting.

Material Parameters for the MEE Plates

The nonlinear analyses for the MEE plate are carried out by considering a bi-layered BaTiO3/CoFe2O4 laminate with various volume fraction (*vf*) of BaTiO3, and the corresponding material properties are presented in Table 2 with 20% offset on the volume fractions.

Table 2. Material parameters for the bi-layered BaTiO3/CoFe2O4 laminates

vf	0%	20%	40%	60%	80%	100%
C_{11}	286	250	225	220	175	166
C_{12}	173	146	125	110	100	77
C_{13}	170	145	125	110	100	78
C_{33}	269.5	240	220	190	170	162
C_{44}	45.3	45	45	45	50	43
e_{31}	0	–2	–3	–3.5	–4	–4.4
e_{33}	0	4	7	11	14	18.6
e_{15}	0	0	0	0	0	11.6
ε_{11}	0.08	0.33	0.8	0.9	1.0	11.2
ε_{33}	0.093	2.5	5.0	7.5	10	12.6
μ_{11}	–5.9	–3.9	–2.5	–15	–0.8	0.05
μ_{33}	1.57	1.33	1.0	0.75	0.5	0.1
q_{31}	580	410	300	200	100	0
q_{33}	700	550	280	260	120	0
q_{15}	560	340	220	180	80	0
d_{11}	0	2.8	4.8	6.0	6.8	0
d_{33}	0	2000	2750	2500	1500	0
ρ_ρ	5300	5400	5500	5600	5700	5800

Unit: elastic constants in 109 N/m2, piezoelectric constants in C/m2, piezomagnetic constants in N/A m2, dielectric constants in 10-9 C2/N m2, magnetic constants in 10-6 N s2/C2, and magnetoelectric coefficients in 10-12 N s/VC.

Verification of the Methodology

To check the validity of the proposed mythology, the first case discussed here is the difference between linear and nonlinear analyses on the MEE plate. Figure 2 illustrates the nonlinear deformation versus linear

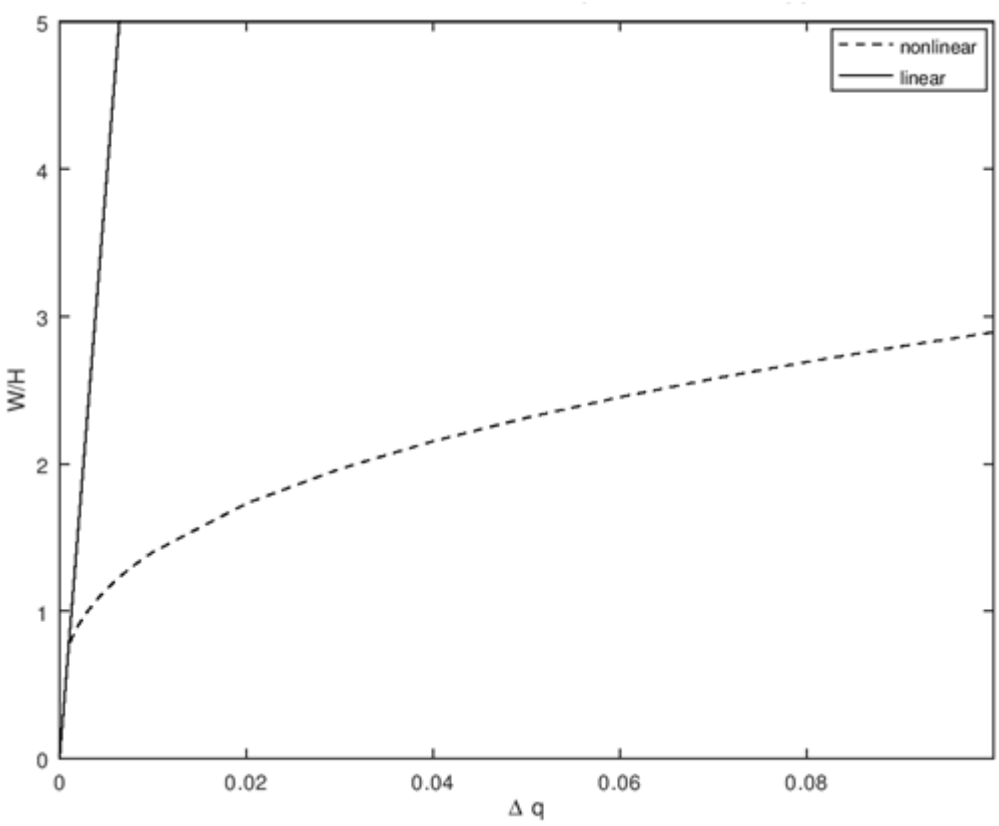

Figure 2. Nonlinear versus linear analyses on the rectangular PZT plate subjected to various strength of applied load

deformation for a simply-supported rectangular MEE plate with respect to various applied loads. Thickness of the plate is set to be 0.05 m, length and width are chosen to be 20 and 10 times the thickness, the volume fraction is 50%, of which the material constants are cited from Table 1 of the literature conducted by Xue *et al.* [2] for comparison purpose.

It should be noted that in Table 1 of the literature [2], magnetoelectric constants are not included, so the authors here used the mean value for 40% volume fraction and 60% volume fraction of the BaTiO3/CoFe2O4 bi-laminates as a reasonable estimate. Also, since in the study of Xue *et al.* [2], only the first mode amplitude is accounted, thus the mode number in this case is set to be $M = N = 1$, that is, the first mode effect is promptly examined through this example.

As we may see from Figure 2, the linear and nonlinear deformations are as expected to be a straight line and a parabola correspondingly. And it is obvious that linear deflection is comparably over-estimated than the nonlinear deflection even when the applied load is in small magnitude, (say less than 0.01). Also, it can be detected that the magnitude of nonlinear deflection is somehow smaller than that presented in the reference paper, with the fact 2.0 versus 4.5 when the applied load density is 0.05. This inconsistency is probably due to the variations in material constants and the adopted algorithms.

Effects of Mode Numbers

Even though first mode effect is conventionally more significant than the other mode in the modal analysis, however, the methodology proposed in this study can actually cope with any value of mode numbers, so the effect of mode numbers on the nonlinear deformation are shown in Figure 3. A simply-

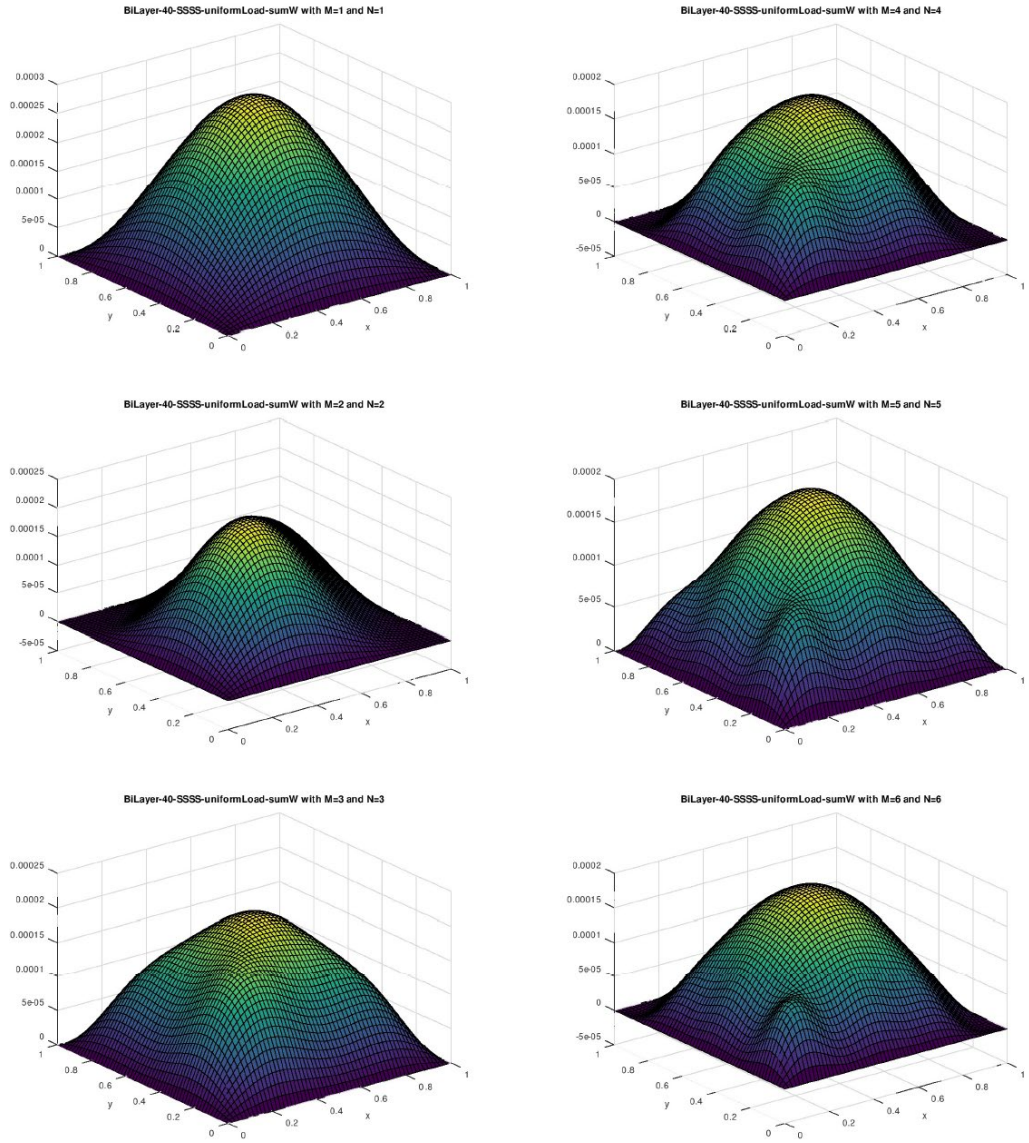

Figure 3. Nonlinear deformation for simply-supported square MEE plate with volume fraction 40% of BaTiO3 with respect to different mode numbers

supported square bi-laminate with length and width both 1m, thickness 0.05 m is considered in this case, and uniform load with magnitude equals to one-tenth of the rigidity (i.e., 0.1*D_E) is applied on the top surface of the MEE plate. The volume fraction is set to be 40%, which is chosen aiming to fully reveal the multiphase property of the MEE plate, and the mode number is increasing from 1 to 6 in order to see the situation with different collecting terms.

From Figure 3, the variances on the nonlinear deformation with respect to different collecting terms can be observed, as the mode number increases we can see the central deformation seems to be decreasing accordingly. Moreover, it can be seen that the accumulated deformation upon the whole plate got several extra hills attached as more collecting terms are made, which is reasonable because the nonlinear terms will result in more perturbation while more modes are aggregated.

Effects of Volume Fractions

In order to see the effect of volume fraction on the deformation of a MEE plate, we investigate the nonlinear deformation of simply-supported square bi-laminates subjected to uniform load with

magnitude fixed as one-tenth of the elastic rigidity, i.e., $\Delta q = 0.1D_E$, for various value of volume fractions. The width and length of the laminate are set to be both 1 m, and the thickness is set to be 1/20 the width, in addition, number of collecting terms are both 3 terms along *x*- and *y*- direction, the maximum deflection of the plate with respect to different volume fractions are depicted in Figure 4.

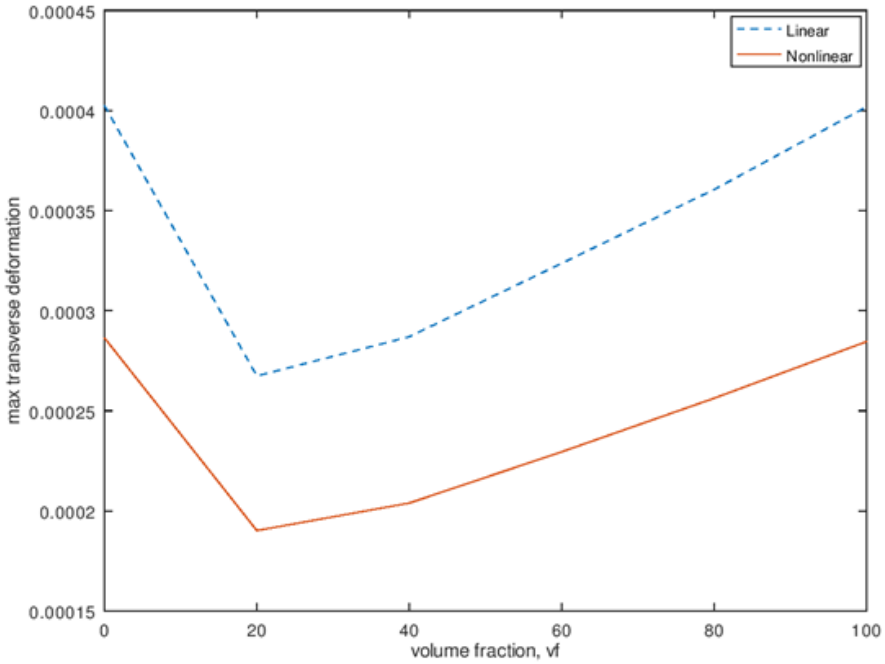

Figure 4. Maximum transverse deflection for simply-supported square MEE plates with various volume fraction

As it may be detected, mechanical loading seems to have less impact on the deformation of multiphase MEE plate, that is, for the two extreme cases, say pure piezoelectric $(vf = 100\%)$ and piezomagnetic $(vf = 0\%)$ plates, it is obvious that the maximum deflections are larger than the other piezoelectric/piezomagnetic coupled plates $(vf = 20\%, 40\%, 60\%)$. So it seems that the equivalent rigidity induced by piezoelectricity/piezomagnetism seems to stabilize the system.

Tip Deformation of The Cantilever MEE Plate Subjected to Impulse Force

As shown in Eq. (14) and Table 1, the formulation of the present study enable the plate to have other boundary conditions in addition to the simply-supported one, thus a rectangular plate with cantilever boundary conditions will be discussed herein in order to demonstrate the applicability.

The width of the laminate is chosen to be 1 m and the length is set to be 0.5 m, whereas the thickness is 0.05 m, and number of collecting terms are set to be both 3. For the cantilever MEE plate, mode shape functions along *x*- and *y*- directions are approximated by

$$X_m(x) = \cosh \alpha_m x - \cos \alpha_m x - \gamma_m(\sinh \alpha_m x - \sin \alpha_m x)$$

and

$$Y_n(y) = \cosh \beta_n y + \cos \beta_n y - \delta_n(\sinh \beta_n x + \sin \beta_n x)$$

where

$$\alpha_1 = 1.875104/L_x,\ \alpha_2 = 4.694091/L_x,\ \alpha_3 = 7.854757/L_x,$$
$$\gamma_1 = 0.734096,\ \gamma_2 = 1.018466,\ \gamma_3 = 0.999225,$$

and

$\beta_1 = 4.730041/L_y$, $\beta_2 = 7.853205/L_y$, $\beta_3 = 10.995607/L_y$,
$\delta_1 = 0.982502$, $\delta_2 = 1.000777$, $\delta_3 = 0.999966$,

in which L_x and L_y denote the width and length of the MEE plate respectively.

An impulse force with magnitude one-tenth of the elastic rigidity is applied at the middle point of the free edge, i.e., $\Delta q = 0.1D_E * delta(x - L_x) * delta(y - L_y/2)$, delta(.) denotes the Dirac delta function. Static deformation of the bi-layered MEE plate with various volume fractions are measured and then summarized in Figure 5 and Figure 6. Figure 5 shows the overall deformation of the MEE laminate with

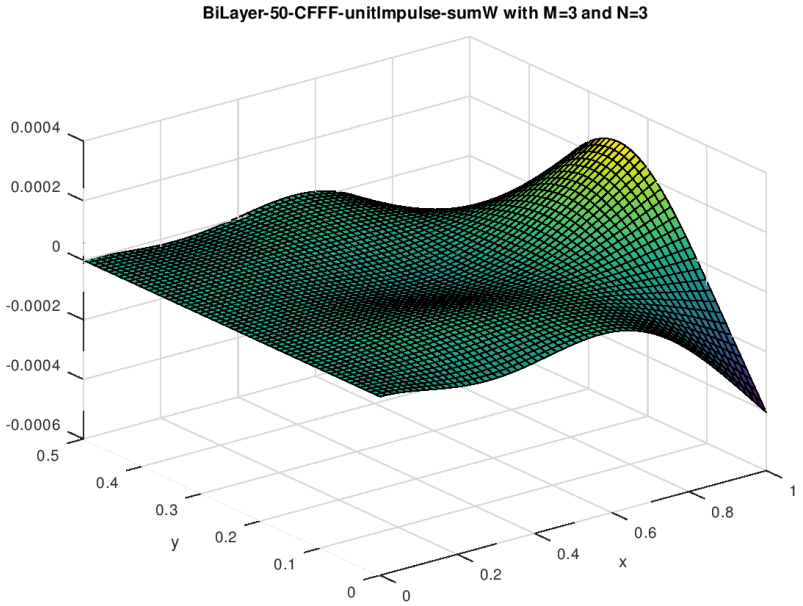

Figure 5. Nonlinear deformation for a Cantilever rectangular equally bi-laminated MEE plate

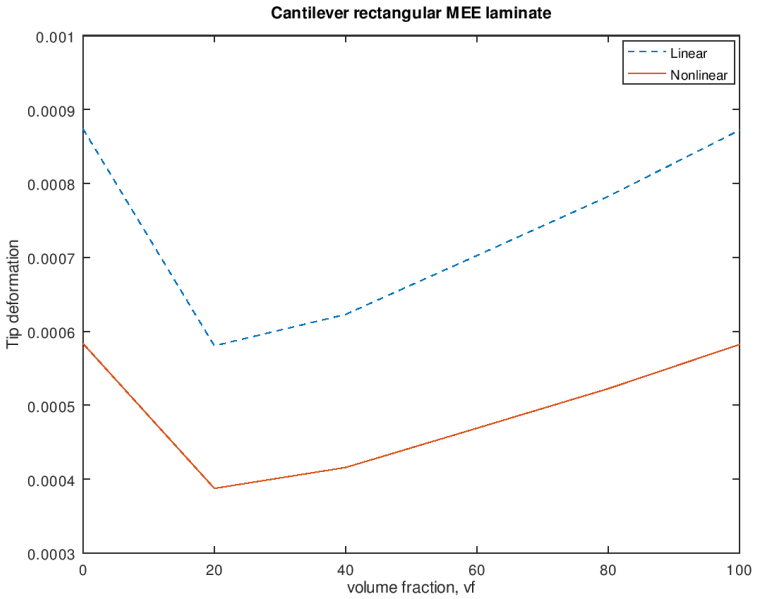

Figure 6. Tip displacement of the Cantilever rectangular MEE plates versus various volume fractions

50% volume fraction, while Figure 6 illustrates the tip deformation of the laminate with respect to various volume fractions.

It can be found from Figure 5 that the maximal deformation might occurs at the point other than the middle point, it could be just at the edge tips. Therefore, the largest deformation for the whole cantilever plate subjected to impulse force are evaluated and depicted in Figure 6 with different volume fraction are considered.

In Figure 6, linear and nonlinear tip deformations of the cantilever MEE laminates are demonstrated, as expected, nonlinear system adds stabilizing factor over the linear system, that is, a less conservative estimate can be found through the nonlinear modelling, so to speak. With the same trend found in Figure 4, MEE laminate with 20% volume fraction seems to be more rigid than the other constitute, a detail investigation should be conducted, future study regarding this issue will be made in near soon.

Conclusions

Mathematical modelling for the large deformation of a magneto-electro-elastic bi-layered laminate is presented in this study. Numerical results are carried out by using the multivariate Newton's method with respect to various volume fractions which refers to volume ratio between piezoelectric and piezomagnetic continua. Verification of the proposed methodology is confirmed, and major conclusions are as follows:

(1) Linear analysis is easier but always produces over-estimate result in compare with the one conducted by nonlinear formulation.
(2) Nonlinearity of the von Karman strain seems to stabilize the system rigidity, so that smaller deformation will be detected when applied load is imposed.
(3) Generally speaking, the multiphase laminate is more rigid than the single-phase continuum. That is, piezoelectricity or piezomagnetizm are actually contributing equivalent rigidities to the whole system.
(4) The effect of volume fraction plays an important role on the nonlinear deformation of the MEE plate. Bi-laminate with 20% of the volume fraction can be found to have greatly reduction on the maximum deformation under applied load.

Conflicts of Interest

The authors declare that there is no conflict of interest regarding the publication of this paper.

Acknowledgement

The financial support from Xiamen University Malaysia Research Fund (XMUMRF) under Grant No. XMUMRF/2018-C2/IMAT0005 received from Mei-Feng Liu and Grant No. XMUMRF/2018-C2/IMAT/0004 received from Liew Siaw Ching are fully acknowledged.

References

[1] Liu, M. F. (2011). An exact deformation analysis for the magneto-electro-elastic fiber-reinforced thin plate. *Applied Mathematical Modelling, 35*, 2443–2461.
[2] Xue, C. X., Pan, E., Zhang, S. Y., & Chu, H. J. (2011). Large deflection of a rectangular magneto-electro-elastic thin plate. *Mechanics Research Communications, 38*, 518–523.
[3] Milazzo, A. (2014). Large deflection of magneto-electro-elastic laminated plates. *Applied Mathematical Modelling, 38*, 1737–1752.
[4] Razavi, S., & Shooshtari, A. (2015). Nonlinear free vibration of magneto-electro-elastic rectangular plates. *Composite Structures, 119*, 377–384.
[5] Nazargah, M. L., & Cheraghi, N. (2017). An exact Peano series solution for bending analysis of imperfect layered FG neutral magneto-electro-elastic plates resting on elastic foundations. *Mechanics of Advanced Materials and Structures, 24*(3), 183–199.
[6] Subhani, S. M., Maniprakash, S., & Arockiarajan, A. (2017). Nonlinear magneto-electro-mechanical response of layered magneto-electric composites: Theoretical and experimental approach. *Acta Mechanica, 228*, 3185–3201.
[7] Biswas, S., & Dahab, S. A. (2020). Electro-magneto-thermoelastic interactions in initially stressed orthotropic medium with Green-Naghdi model type-III. *Mechanics Based Design of Structures and Machines, 50*(1), 1–

16.
[8] Reddy, J. N. (2003). *Mechanics of laminated composite plates and shells: Theory and analysis* (2nd ed.). Boca Raton, FL: CRC Press.
[9] Tzou, H. S. (1993). *Piezoelectric shells: Distributed sensing and control of continua*. Netherlands: Springer.
[10] Burden, R. L., & Faires, J. D. (2011). *Numerical analysis* (9th ed.). Boston, MA: Brooks/Cole.

Appendix A. Algorithm for Multivariate Newton's Method

To approximate the solution of the nonlinear system $\mathbf{F}(\mathbf{x}) = \mathbf{0}$ given an initial approximation $\mathbf{x}$:
INPUT number *n* of equations and unknowns; initial approximation $\mathbf{x} = (x_{1,\ldots,}x_n)^t$, tolerance *TOL*; maximum number of iterations *N*.
OUTPUT approximate solution $\mathbf{x} = (x_{1,\ldots,}x_n)^t$ or a message that the number of iterations was exceeded.

Step 1 Set $k = 1$.
Step 2 While $(k \leq N)$ do steps $3 - 7$.
Step 3 Calculate $\mathbf{F}(\mathbf{x})$ and $J(\mathbf{x})$, where $J(\mathbf{x})_{i,j} = \left(\partial f_i(\mathbf{x})/\partial x_j\right)$ for $1 \leq i, j \leq n$.
Step 4 Solve the $n \times n$ linear system $J(\mathbf{x})\mathbf{y} = -\mathbf{F}(\mathbf{x})$.
Step 5 Set $\mathbf{x} = \mathbf{x} + \mathbf{y}$.
Step 6 If $\|\mathbf{y}\| < TOL$ then OUTPUT $(\mathbf{x})$;
(*The procedure was successful*.)
STOP.
Step 7 Set $k = k + 1$.
Step 8 OUTPUT ('Maximum number of iterations exceeded');
(*The procedure was unsuccessful*.)
STOP.